A new track inspection car based on a laser camera system

Shengwei Ren (任盛伟)[1,2], Shiping Gu (顾世平)[2], Guiyang Xu (许贵阳)[2], Zhan Gao (高 瞻)[1], and Qibo Feng (冯其波)[1*]

[1]*Institute of Optoelectronic Measurement and Control Technology, Beijing Jiaotong University, Beijing 100044, China*

[2]*Infrastructure Inspection Center, Ministry of China Railway, Beijing 100081, China*

[*]*Corresponding author: qbfeng@bjtu.edu.cn*

Received August 5, 2010; accepted November 24, 2010; posted online February 24, 2011

We develop and build a new type of inspection car. A beam that is not rigidly connected to the train axle boxes and can absorb the vibration and impact caused by the high speed train is used, and a laser-camera measurement system based on the machine vision method is adopted. This method projects structural light onto the track and measures gauge and longitudinal irregularity. The measurement principle and model are discussed. Through numerous practical experiments, the rebuilt car is found to considerably eliminate the measurement errors caused by vibration and impact, thereby increasing measurement stability under high speeds. This new kind of inspection cars have been used in several Chinese administration bureaus.

OCIS codes: 120.0120, 100.0100, 150.0150.

doi: 10.3788/COL201109.031202.

Rail track geometric parameters, such as gage, level, twist, longitudinal irregularity, and alignment irregularity, etc., have much influence on the operation safety of trains[1−6]. With the development of Chinese railroads, train speed has rapidly improved, causing exceedingly serious track abrasions. Thus, developing a precise, efficient, and economical track geometric parameter measurement system has become a serious concern. The hanging beam is currently used in the China GJ-4 type track inspection car, and a similar measurement system has been adopted in Italy as well[7]. The entire hanging beam is installed on the longitudinal beam, which is rigidly connected to the train axle boxes. The displacement meters are installed inside the hanging beam to measure gauge, longitudinal irregularity, and alignment irregularity. In this measurement system, shock absorption mechanisms cannot be installed because of its measurement principle. In other words, the hanging beam and train axle boxes must be rigid as a whole. However, with the rapid development of high speed railways in China, track inspection car speeds have also rapidly increased, causing stronger impact and vibration to the hanging beam. This, in turn, significantly decreases measurement accuracy. With increasing speeds, the hanging beam can even break. This type of track inspection car cannot work properly at train speeds of up to 120 km/h[8,9]. Now, machine vision technology is more frequently applied in the measurement field, and has also been widely used in track inspection cars abroad[10−14]. For example, this technology is used in the Korean Train Express rail inspection measurement system[15]. However, determining technical details in this technology is difficult. Hence, developing a new track inspection car that will satisfy the specific requirements and accommodate rapid developments in Chinese high speed railways is essential.

The layout of the proposed new system is shown in Fig. 1. A mechanism for absorbing vibration and impact is adopted, and a new system using machine vision (Fig. 2) and the inertia system for measuring the track geometric parameters are used. As shown in Fig. 2, when structural light is projected onto the track by the laser, the images of the rail profile can be captured by the charge-coupled device (CCD) camera, and the displacement between the vertex of the rail and the CCD camera can be measured in real time through fast image processing.

The model for measuring track geometric parameters is shown in Fig. 3. G, generally having a value of 1500 mm, is the standard distance between the midpoint of the left and right tracks. L, which is a constant value, is the distance between the left and right cameras.

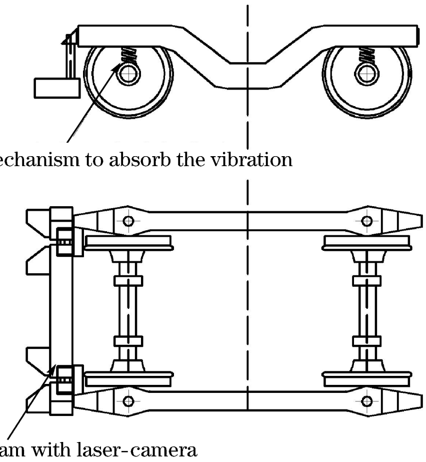

Fig. 1. Layout of the beam with laser-camera.

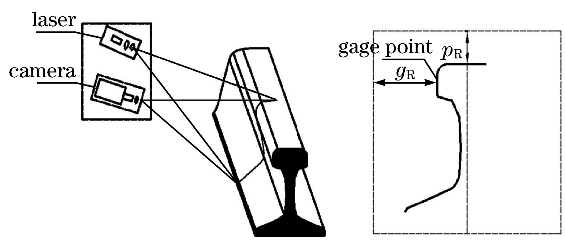

Fig. 2. Basic track gauge measurement principle by machine vision.

g_R is the distance between the track and the right camera, g_L is the distance between the track and the left camera, P_R is the vertical distance between the vertex of the right track and the beam, and P_L is the vertical distance between the vertex of the left track and the beam. These four parameters can be measured by the laser camera system. a_y is the lateral acceleration of the midpoint on the beam, z_R and z_L are the Z coordinates of the vertex of the left and right tracks, respectively; z_{cr} and z_{cl} are the Z coordinates of the car floor above the left and right track top surfaces, respectively; and y_R and y_L are the Y coordinates of the gauge points of the left and right tracks, respectively. These parameters are the values of alignment irregularity to be measured. y_b is the Y coordinate of the middle point of the beam, and z_b is the Z coordinate of the middle point of the beam. The following equations can be obtained from Fig. 3:

$$g = g_R + g_L + L, \tag{1}$$

$$g_L = y_b - y_L - L/2, \tag{2}$$

$$g_R = y_R - y_b - L/2, \tag{3}$$

where y_b can be measured indirectly by the inertia sensor through the following procedures.

The height difference of the left and right tracks can be expressed as Θ_t

$$\Theta_t \equiv \frac{z_R - z_L}{G}. \tag{4}$$

The inclination angle of the car body can be express as

$$\Theta_c \equiv \frac{z_{cr} - z_{cl}}{G}. \tag{5}$$

From the geometric relationship shown in Fig. 3, we obtain

$$P_L = z_L - z_b + 1/2G\ \Theta_b, \tag{6}$$

$$P_R = z_R - z_b - 1/2G\ \Theta_b, \tag{7}$$

where Θ_b is the inclination angle of the beam. From Eqs. (4) and (5), we have

$$\Theta_t = \Theta_c - \frac{d_{cl} - d_{cr}}{G}. \tag{8}$$

Similarly, from Eqs. (6) and (7), we obtain

$$\Theta_b = \Theta_t + \frac{P_L - P_R}{G}, \tag{9}$$

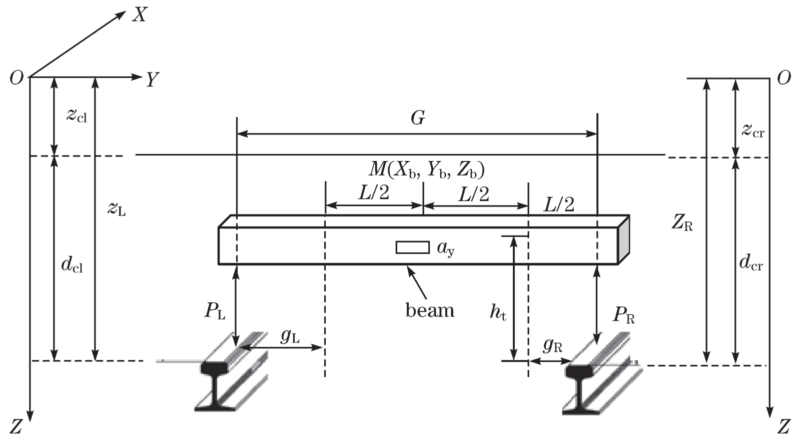

Fig. 3. Measurement principle of longitudinal irregularity.

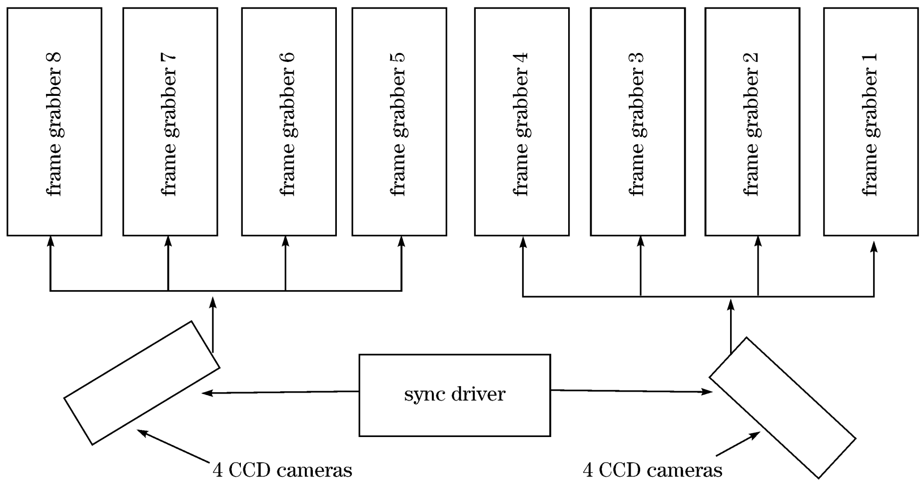

Fig. 4. Image sampling diagram.

Table 1. Comparison between Car-Measured and Hand-Measured Values

Sequence Number	Position	Geometric Irregularity	Value Measured by the Car (mm)	Value Measured by Hand (mm)	Difference (mm)
1	694 km+848 m	Gauge	8.3	8	0.3
2	693 km+955 m	Gauge	6	5	1
3	693 km+956 m	Left AI	7	6	1
4	522 km+011 m	Right AI	12	11	1
5	1236 km+410 m	Left LI	−16	−15	−1
6	1115 km+652 m	Right LI	−22	−21	−1
7	1115 km+628 m	Right LI	−16	−17	1
8	369 km+680 m	Right LI	−6	−5	−1
9	369 km+633 m	Gauge	−5	−4	−1
10	369 km+462 m	Left LI	6	5	1

AI: alignment irregularity; LI: longitudinal irregularity

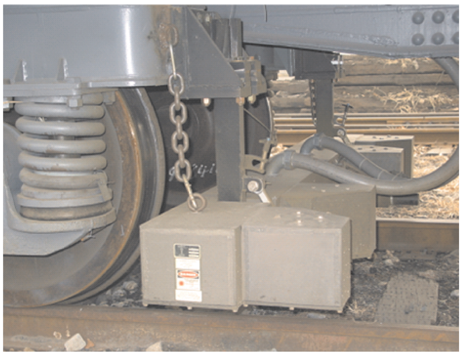

Fig. 5. Laser-camera system.

where the inclination Θ_c of the car body can be measured by the inertia sensor, the Θ_t and Θ_b can be obtained from Eqs. (8) and (9), and y_b can be obtained by

$$\frac{d^2 y_b}{dt^2} = a_y + g \sin \Theta_b - h_t \frac{d^2 \Theta_b}{dt^2}, \qquad (10)$$

where h_t is the height of the sensitive axis of the lateral accelerometer above the gauge plane of the rail. The first item on the right side of Eq. (10) is the lateral acceleration of the beam; the second item is the component of the gravity force; and the third item is the acceleration at which the beam rotates along with its center axis. These three items can be measured by the sensors.

The longitudinal irregularity can be measured in a similar manner. As shown in Fig. 4, the entire laser-camera system mainly consists of two laser light sources, eight CCD cameras, and video processing sub-systems that include the frame grabber and field-programmable gate array (FPGA). The frame grabber, FPGA image measurement card, and computer are installed on the 19-inch cabinet on the car. The image of this laser-camera system is shown in Fig. 5. The laser with a wavelength of 808 nm was used and the laser power is 2 W; the CS8620HI camera from Toshiba was adopted. The camera had a pixel number of 768 (H) $\times$ 494 (V) (pixels); the measurement range for the camera was 300 (H) $\times$ 200 (V) (mm); and the resolution was about 0.4 mm.

To enhance the sampling rate, the eight cameras and frame grabbers were used and divided into two groups, which were used to simultaneously measure the left and right rails. The image processing speed of each frame grabber is 60 frames/s. The sampling time delay between neighboring CCD cameras is 0.25 s. In this way, the sampling rate can be enhanced to 240 frames/s.

The work flow of the laser-camera subsystem is shown in Fig. 6. The measured track is illuminated by the structural light from the laser, then the cross-section contour of the track is obtained, and the corresponding geometric parameters are measured through image measurement.

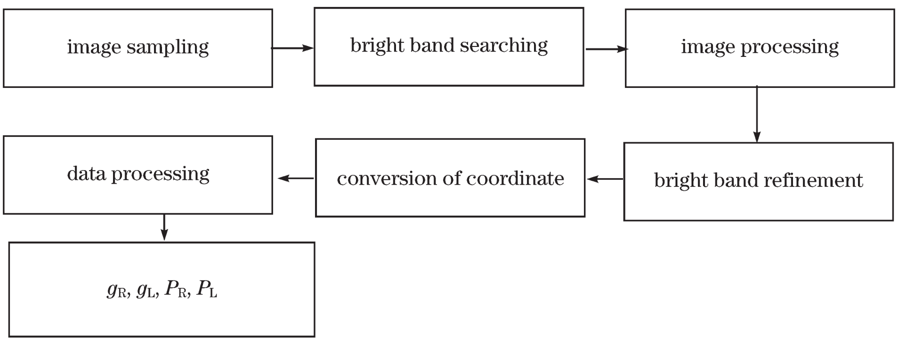

Fig. 6. Image processing flowchart.

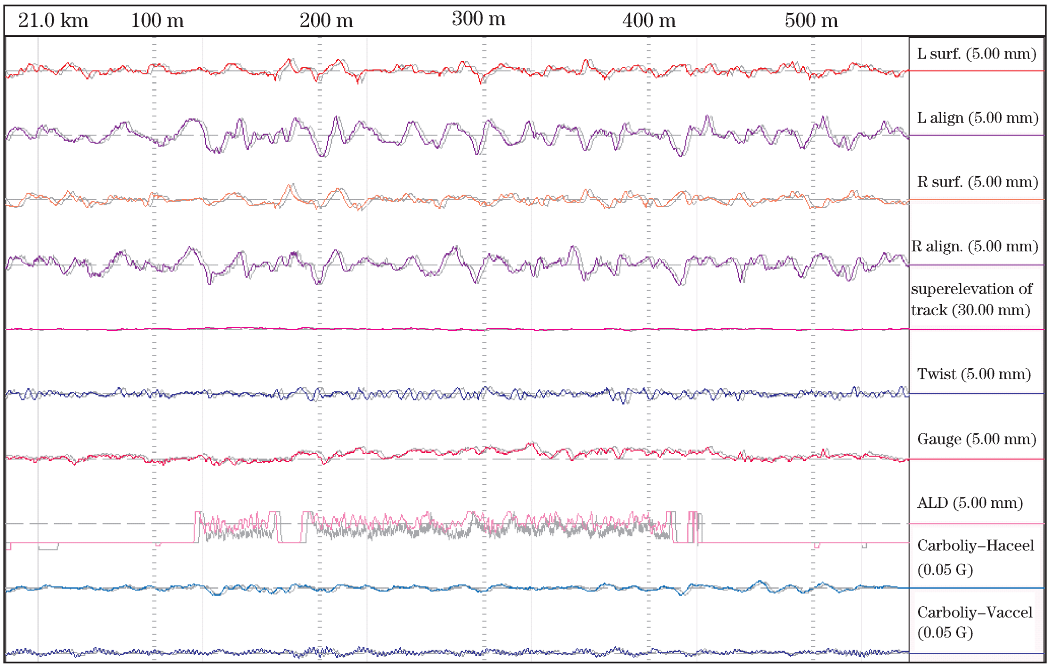

Fig. 7. Repetitive measurement results. L surf.: left rails surface irregularity; R surf.: right rails surface irregularity; L align.: left rail align irregularity; R align.: right rail align irregularity; ALD: automatic location detection.

To verify the performance of this new track inspection car, we carried out several outfield experiments on different sites on the Longhai Line. Table 1 shows the track geometric parameter comparison results. From this table, we can see that the maximum difference between the measured value yielded by our system and that generated by hand is 1 mm.

Some repetitive experimental results conducted using a train speed of 160 km/h are shown in Fig. 7, which illustrates that the measurement accuracy of gauge and alignment irregularity is 0.4 and 0.8 mm, respectively. Compared with the old track inspection car, the new inspection car exhibits good repeatability.

In conclusion, a new GJ-4G track inspection car is developed and a laser-camera sub-system is adopted to replace the hanging beam of the old track inspection car—an approach that can eliminate the measurement errors caused by vibration and impact, thereby improving measurement stability. Currently, six GJ-4G inspection cars are being used in six different railway administration bureaus and provide safety for the operation of Chinese railways.

This work was supported by the National "863" Program of China under Grant No. 2009AA11Z102-1.

References

1. T. Hirofumi and F. Atsushi, Railway Technical Research Institute **50,** 116 (2009).
2. P. F. Weston, C. S. Ling, C. Roberts, C. J. Goodman, P. Li, and R. M. Goodall, Journal of Rail and Rapid Transit **221,** 75 (2007).
3. D. Li, A. Meddah, K. Hass, and S. Kalay, in Proceedings of the Institution of Mechanical Engineers **220,** 273 (2006).
4. D. Chai, S. Wei, L. Xia, G. Fan, L. Liu, and A. Yang, China Railway Science (in Chinese) **25,** 35 (2004).
5. E. G. Berggren, M. X. D. Li, and J. Spannar, Wear **265,** 1488 (2008).
6. J. Madejski, Journal of Materials Processing Technology **157,** 194 (2004).
7. M. Bocciolone, A. Caprioli, A. Cigada, and A. Collina, Mechanical Systems and Signal Processing **211,** 242 (2007).
8. S. Wei, L. Liu, W. Liu, and S. Jiang, China Railway Science (in Chinese) **31,** 143 (2010).
9. L. Wu, S. Xiao, and F. Xu, Railway Vehicle (in Chinese) **47,** 18 (2009).
10. Y. Xu, Y. Jiang, and F. Chen, Acta Opt. Sin. (in Chinese) **29,** 72 (2009).
11. D. V. Popov, R. B. Ryabichenko, and E. A. Krivosheina, Proc. SPIE **5920,** 15 (2005).
12. J. Zhu, X. Li, and Y. Xu, Acta Opt. Sin. (in Chinese) **30,** 1297 (2010).
13. D. V. Popov and R. B. Ryabichenko, Proc. SPIE **5580,** 367 (2005).
14. B. He and X. Zhou, Chinese J. Lasers (in Chinese) **37,** 1618 (2010).
15. S. Kim, C. Park, Y. Kim, and C. Park, Journal of Mechanical Science and Technology **23,** 1019 (2009).